Ruiz-Ruano, F. J., Navarro-Domínguez, B., Camacho, J. P. M., & Garrido-Ramos, M. A. (2019). Characterization of the satellitome in lower vascular plants: The case of the endangered fern Vandenboschia speciosa. Annals of Botany, 123(4), 587-599.

is available online at:
https://academic.oup.com/aob/article/123/4/587/5142925

DOI: 10.1093/aob/mcy192

Characterization of the satellitome in lower vascular plants: the case of the endangered fern *Vandenboschia speciosa*

Ruiz-Ruano F.J.; Navarro-Domínguez, B.; Camacho J.P.M.; Garrido-Ramos M.A.
Departamento de Genética, Facultad de Ciencias, Universidad de Granada, Granada, Spain

Correspondence:

Dr. Manuel A. Garrido-Ramos
Departamento de Genética
Facultad de Ciencias
Universidad de Granada
Avda. Fuentenueva s/n, 18071
Granada, Spain
Phone number: 958249710
Fax number: 958244073
e-mail: mgarrido@ugr.es

Abstract

Background and Aims: *Vandenboschia speciosa* is a highly vulnerable fern species, with a large genome (10.5 Gb). Haploid gametophytes and diploid sporophytes are perennial, can reproduce vegetatively, and certain populations are composed only of independent gametophytes. These features make this fern a good model: i) for high-throughput analysis of satellite DNA (satDNA) to investigate possible evolutionary trends in satDNA sequence features; ii) to determine the relative contribution of satDNA and other repetitive DNAs to its large genome; and iii) to analyze whether reproduction mode or phase alternation between long lasting haploid and diploid stages influence satDNA abundance or divergence.

Methods: We analyzed the repetitive fraction of the genome of this species in three different populations (one composed only by independent gametophytes), using Illumina sequencing and bioinformatic analysis with RepeatExplorer and satMiner.

Key Results: The satellitome of *V. speciosa* is composed of eleven satDNA families, most of them showing short repeat length and being A+T rich. Some satDNAs had complex repeats composed of sub-repeats, showing high similarity with shorter satDNAs. Three families had particular structural features and highly conserved motifs. satDNA only amounts ~0.4% of its genome. Likewise, microsatellites don't represent more than 2%, but TEs represent ~50% of the sporophytic genomes. We found high resemblance in satDNA abundance and divergence both between gametophyte and sporophyte samples from a same population and between populations.

Conclusions: i) Longer (and older) satellites in *V. speciosa* have higher A+T content and evolve from shorter ones and, in some cases, microsatellites were a source for new satDNAs; ii) the satellitome doesn't explain the huge genome size in this species while TEs are the major repetitive component of *V. speciosa* genome and mostly contributes to its large genome; iii) reproduction mode or phase alternation between gametophyte and sporophyte doesn't entail accumulation or divergence of satellites.

Introduction

Eukaryotic genomes contain large amounts of different classes of repetitive DNA sequences either arranged in tandem or dispersed (López-Flores and Garrido-Ramos, 2012; Biscotti et al., 2015). Among tandem repetitive DNA, moderately repetitive DNAs includes ribosomal RNA (rRNA) and protein-coding gene families or short tandem telomeric repeats, while highly repetitive DNA includes non-coding microsatellite and satellite DNA (satDNA), including centromeric DNA. Among dispersed repeats, transposable elements (TEs) such as DNA transposons and retrotransposons (mainly LTR retrotransposons and non-LTR retrotransposon or LINEs) constitute a main fraction of highly repetitive DNA, also including SINEs (moderately to highly repetitive DNA), retrogenes and retropseudogenes as well as several gene families composed of dispersed members (moderately repetitive DNA).

Repetitive DNA largely contributes to pronounced differences in genome size between species (López-Flores and Garrido-Ramos, 2012; Biscotti et al., 2015). Among repetitive sequences, TEs are mostly responsible for these differences and retrotransposons are the most abundant with a predominant presence of LTR-retrotransposons in plants (López-Flores and Garrido-Ramos, 2012; Biscotti et al., 2015). Notwithstanding, satDNA also contributes greatly to genome size variation in some organisms (Plohl et al., 2012; Garrido-Ramos, 2015, 2017). While the repeatome (Kim et al., 2014) is the whole collection of repetitive DNA, the satellitome is the whole collection of different satDNA families in a genome (Ruiz-Ruano et al., 2016). For decades, access to satDNA families of the satellitome was based on the isolation from restriction endonuclease treatment of genomic DNA, a method that simplified and popularized the study of satDNA, but that have several drawbacks (reviewed in Garrido-Ramos, 2017). Today, Next Generation Sequencing (NGS) and high-throughput *in silico* analysis of the information contained in NGS reads have revolutionized the study of this an other repetitive fractions of eukaryotic genomes (Novák et al., 2010, 2013; Weiss-Schneeweiss et al., 2015).

For this purpose,, an efficient pipeline called RepeatExplorer was developed by Novák et al. (2010, 2013) which allows for the *de novo* identification of repetitive DNA families in species lacking a reference genome, thus facilitating the analysis of both the repeatome (Kim et al., 2014), in general, and the satellitome (Ruiz-Ruano et al., 2016), in particular. Afterwards, Ruiz-Ruano et al. (2016) implemented a bioinformatic toolkit (satMiner), based on consecutive rounds of clustering of Illumina reads by RepeatExplorer, which allows identification of satDNA families, alternating with filtering out of the already known families thus increasing the

likelihood of finding new rare satDNA families. This toolkit has proven being useful in species with high C-value and/or small amount of satDNA (Ruiz-Ruano et al, 2016). In addition, Novák et al. (2017) developed Tandem Repeat Analyzer (TAREAN), a further improvement of RepeatExplorer which allows the automatic identification of satDNA repeats and reconstruction of representative monomer sequences for each satDNA family (Novák et al., 2017). All these genomic approaches are being used last years for the analysis of TEs and satDNA content in many species, and provide an opportunity to uncover satDNA families whose isolation was elusive by other methods. Thus, the combination of NGS and computer analysis favours an in-depth global genomic analysis of the satellitome by uncovering the different satDNA families making up a given genome, their relative abundance and variability, the core details of their evolution, as well as their roles in different genetic and genomic processes (Weiss-Schneeweiss et al., 2015). In addition, this new perspective greatly contributes to the development of comparative genomics and phylogenomics (Weiss-Schneeweiss et al., 2015).

Vandenboschia speciosa (Willd.) G. Kunkel (= *Trichomanes speciosum* Willd.) is a fern species of the family Hymenophyllaceae, with a genome size of 10.496 Gb (Obermayer et al., 2002). *V. speciosa* is an endangered rare European-Macaronesian endemism, the only representative of a genus which has a primarily tropical distribution, restricted to disjoined regions of the European Atlantic coast and the Macaronesian islands (Canaries, Madeira and Azores). The two phases of *V. speciosa* life cycle are perennial and can reproduce by vegetative propagation (Rumsey et al., 1999). The "floaty" sporophyte (fronds made of a translucent single layer of cells) is rhizomatous and can spread by fragmentation of the rhizome. The gametophyte, unlike a heart-shaped prothallus, is epigeous and narrowly filamentous with specialized asexual propagules (gemmae), and can survive in some populations during long periods outside the range of sporophyte distribution (Rumsey et al, 1999). In the warmer climatic conditions in the South of the Iberian Peninsula and Macaronesian islands this species usually undergoes a normal fern lifecycle of two free-living generations but, as one goes further north and east Europe, the sporophyte generation becomes increasingly rare (Rumsey et al, 1999). However, one out of eight populations of this species located in the south of the Iberian Peninsula shows only the gametophyte phase, which propagates vegetatively.

These biological, life-history and genomic features, together with the phylogenetic position of ferns within vascular plants, make this species an attractive species for satellitome analysis. This part of the genome has been elusive during years in *V. speciosa* by conventional methods (Garrido-Ramos, personal observation). Here, we analyze four genomic libraries

belonging to three different populations of this species, two of them showing alternation of haplo- and diploid generations and the other being composed only by haploid independent gametophytes. Our aim was to characterize the different satDNA families contributing to the satellitome of *V. speciosa*, to assess the relative contribution of satDNA to the large genome of *V. speciosa* in comparison with other repetitive DNAs, and to ascertain whether the amount or divergence of satDNA change between sporophytic and gametophytic stages or might be influenced by the mode of reproduction.

Materials and Methods

Materials

Vandenboschia speciosa specimens were collected at three populations located in the Alcornocales Natural Park (Cádiz, Spain): Canuto de Ojén-Quesada (OJEN); Valdeinfierno (VALD), and La Almoraima (ALMO). Samples were: OJENs (sporophyte phase from OJEN population), VALDs (sporophyte phase from VALD population), VALDg (gametophyte phase from VALD population), and ALMOg (gametophyte phase from ALMO population). While OJEN and VALD are two populations where this species alternates between the sporophyte and the gametophyte phases, ALMO is composed only of gametophytes. Sporophytes were frozen in liquid nitrogen in the field. Patches with gametophytes were taken in a Petri dish with soil to the laboratory where, under a binocular microscope, the filaments were separated one by one from the soil and from other visible plant and animal species, cleaned, and frozen in liquid nitrogen. All samples were stored at −80 °C and genomic DNA (gDNA) was isolated from each population using the DNeasy plant Mini kit (Quiagen). Pools of DNAs were generated from sets of five specimen DNAs and separated Next Generation Sequencing of the samples was carried out based on the Illumina HiSeq 2000 PE 2x101 nt for OJENs, VALDs and ALMOg, and on the Illumina HiSeq X Ten PE 2x151 nt for VALDg.yielding about 8 Gb (~0.75x coverage) data for VALDs, ALMOg, VALDg and about 16 Gb (~1.5x coverage) for OJENs. Illumina sequencing data can be accessed at SRA-Genbank database in the BioProject PRJNA387541.

SatDNA mining

We applied the protocol satMiner (Ruiz-Ruano et al., 2016), which is based in consecutive rounds of clustering of Illumina reads by RepeatExplorer (Novák et al., 2013), using a subset of reads (100,000 per library), and subsequent filtering of the already assembled reads using DeconSeq (Schmieder and Edwards, 2011), in order to solve the computational problems of handling large datasets with RepeatExplorer.

We performed a quality trimming with Trimomatic (Bolger et al., 2014), and randomly selected 2x100,000 Illumina reads with SeqTK (https://github.com/lh3/seqtk), to run RepeatExplorer with default options. Clusters with spherical or ring-shaped structure and density values higher than 0.1 are likely satDNA, and they were manually selected and inspected for tandem repeats using the dotplot tool in Geneious v4.8 (Drummond et al., 2009). The contigs with higher coverage were then split in monomers and aligned in order to generate a consensus monomer for each satDNA cluster.

We filtered out the reads showing homology with the already clustered contigs and the already identified satDNA using DeconSeq, and selected a new set of 2x100,000 reads from the filtered libraries, that were clustered with RepeatExplorer in a second round. This allows detecting satDNAs being poorly represented in the raw reads. We repeated the filtering using the clusters in the second round, and selected 2x300,000 reads for a third round. We repeated the process two more times adding 2x600,000 reads each time, but no new satDNA was detected further than the third round. This protocol was first performed in OJEN population, were we got consensus sequences for 11 satDNA. Later, we performed a similar analysis in the libraries from VALD and ALMO, adding the consensus of the satDNA sequences already known as a custom database in RepeatExplorer, in order to annotate them if the same satDNA was present in these two populations and also to detect whether new ring-shaped or spherical clusters (i.e. graph shape for satDNA) were specific to any of them.

SatDNA sequence analysis

To detect a representative number of sequences for each satDNA in each population, we selected the reads showing homology with the catalogue of satDNAs identified, using BLAT (Kent 2002), as implemented in a custom script (https://github.com/fjruizruano/ngs-protocols/blob/master/mapping_blat_gs.py), and selected 2x10,000 reads from each population to run RepeatExplorer clustering using a custom database for annotating the sequences of all assembled satDNAs. The BLAT parameters we applied were -stepSize=5 -repMatch=2253 -minScore=0 -minIdentity=0.

None of the satDNAs contained telomere-like repeats. As TTTAGGG has been described as the telomere sequence for several species of pteridophytes (Suzuki 2013), we performed a literal search of TTTAGGG in the raw reads using the grep tool (a command-line software to search for lines with a given pattern in plain-text data sets). Then, we selected those reads where this TTTAGGG was repeated. Alignments and comparison between populations was performed using 10 repeats.

In addition, we estimated the abundance for short satDNAs with monomer length between 1 to 6 nt, also known as microsatellites, using RepeatMaksker with the "-int" option.

Abundance and divergence for each satDNA in each population was calculated with RepeatMasker (Smit et al., 2015) with the crossmatch search engine, mapping 2 x 5,000,000 reads from each population to the satDNA consensus sequences and $(TTTAGGG)_{30}$ for the analysis for the telomeric repeats.

Repeat monomers were extracted from the reads and aligned, in order to perform sequence comparisons between populations. In case of satDNAs with repeat unit length shorter than 101 nt, monomers were directly extracted from Illumina reads sequence. When repeat unit length surpassed read length, we used read pairs where the paired reads overlapped. MEGA v.6 (Tamura et al., 2013) was used to estimate intra-population genetic variation and inter-population divergence as well for phylogenetic analysis. Comparison between satDNA families were performed with the RepeatMasker method described below.

The EMBOSS suite of bioinformatics tools (Rice et al., 2000) was used for the detection of internal repeats (direct or inverted) as well as palindromes. The programs used from the package were MATCHER, ETANDEM, EINVERTED, POLYDOT and PALINDROME. Secondary structure estimation for repeat sequences with shorter inverted repeats and palindromes was made by using the RNAstructure Predict a Secondary Structure Web Server (Reuter and Mathews, 2010).

Our study also included an analysis of nucleotide diversity (π) per position for every satDNA using the sliding windows option of the DnaSP v.5.10 program (Librado and Rozas, 2009). Geneious v4.8 (Drummond et al., 2009) was used to generate sequence logos to convey level of sequence divergence and display conserved motives revealed by the DnaSP program.

The bendability/curvature propensity plots were made with the bend.it server (Vlahovicek et al., 2003), using the DNase I based bendability parameters of Brukner et al. (1995) and the consensus bendability scale (Gabrielian and Pongor, 1996).

TE characterization from Illumina reads

The use of the RepeatExplorer pipeline (Novák et al., 2013) allowed us to additionally characterize the TE content of the *V. speciosa* genome. Repeat identification by a single similarity-based clustering of 250,000 read pairs from each of the two sporophyte libraries (1,000,000 reads in total) was performed using the RepeatExplorer pipeline. This software employs graph representation of read similarities to identify clusters of frequently overlapping reads representing various repetitive elements or their parts (Novák et al., 2010) and provides

248 comparative information about repeat quantities estimated from the number of reads for each
249 library in a cluster. In addition, it performed an annotation based on similarity searches to the
250 RepeatMasker Viridiplantae database of repetitive elements.
251
252 ***Gametophyte contamination analysis***
253 Since gametophytes are found in the ground in tight contact with stream water, DNA
254 extracted from them can conceivably be excessively contaminated by microorganisms, even
255 after careful cleaning. This contamination might bias satDNA abundance estimations in the
256 gDNA libraries. For this reason, we checked the degree of contamination of every sample using
257 the RNA-Seq Illumina sequencing data from a Valdeinfierno sporophyte and a gametophyte,
258 previously used in Ruiz-Estévez et al. (2017a, b). We assembled separately the two
259 transcriptomes using the Trinity v.2.5 *de novo* assembler (Haas et al., 2013) after trimming and
260 *in silico* normalization under default options. Finally, we built SuperTranscripts to get a unique
261 sequence per sequence graph using the Trinity's tool.
262 We annotated the contigs for both assemblies using the Trinotate v.5 software
263 (https://trinotate.github.io/) using the SwissProt database (Bairoch and Apweiler, 2000) and
264 aligning with BLASTX (Altschul et al., 1997). Then we compared the annotation terms between
265 sporophyte and gametophyte to generate two pools of sequences: a) a random selection of
266 500 sporophyte transcriptomic contigs with an annotation also found in the gametophyte
267 transcriptome, and b) a selection of the gametophyte transcriptomic contigs annotated with a
268 term being absent in the sporophyte transcriptome and, in addition, showing mappings in the
269 two gametophytic genomic libraries, using SSAHA2. To assign the most similar species to the
270 sequences in these two pools, we annotated them with Blast2GO (Conesa et al., 2005) against
271 NR database using BLASTX.
272 As we found a high level of contaminants in the gametophyte assembly, we designed
273 an analysis to calculate the degree of contamination in the gametophyte libraries in order to
274 estimate coefficients to correct satDNA abundance quantification in the gDNA libraries. For
275 this purpose, we first selected, in the sporophyte transcriptome, those CDSs being longer than
276 3000 nt, in order to reduce bias due to the low coverage of gDNA libraries. Then we mapped
277 the gDNA reads of the four *V. speciosa* libraries against these long CDS references, using
278 SSAHA2 software (http://www.sanger.ac.uk/science/tools/ssaha2-0). This allowed estimating
279 an approximate number of copies for each contig and library, using the protocol applied by
280 Navarro-Dominguez et al. (2017), with 99% minimum mapping identity for the SSAHA2
281 software to avoid mapping of the contaminant reads. To delimit this analysis to genes showing

a single copy per haploid genome, we restricted it to those contigs showing average copy number in the sporophytes (OJENs and VALDs) lying between 0.7 and 1.3. We then calculated average copy number per library and normalized them in respect to OJENs, i.e. the library showing the highest value. We finally used the resulting coefficients to correct satDNA abundance estimates in the gDNA libraries.

Statistical analyses

Shapiro-Wilk's W test showed that the observed variation for unit length, A+T content, abundance and divergence in all populations fitted a normal distribution (Table S1), for which reason we used parametric statistical tests, such as Pearson correlation analysis and Student t-test for dependent samples, using Statistica (Statsoft Inc.). Comparisons of satDNA abundance and divergence between genomic libraries were performed by the non-parametric Friedman ANOVA.

Results

High-throughput search for satDNA

After the first run of RepeatExplorer (RE) analysis and three additional runs of filtering+RE, performed on the OJENs library, we found 11 satDNAs, defined by monomer length and sequence (Table 1 and Figure S1). Figure S2 shows the reconstruction of representative monomer sequences for each satDNA family. These sequences are deposited in the GenBank database under accession numbers MH048647-MH048657. The same 11 satDNAs were identified independently in the VALDs, VALDg and ALMOg libraries. SatDNA sequences showed no homology with any other DNA sequence deposited in DNA databases (BLAST search found no significant similarity with any other DNA sequence). Table 1 shows the main features of these satDNAs. Their repeat units were short in length (between 32 and 141 bp), with eight satDNAs being shorter than 100 bp. Likewise, most of them were A+T rich, with seven satDNAs showing this parameter between 56.6% and 70.0%, three between 51.1% and 52.7% A+T, and only one actually being G+C rich by showing 45.4% A+T content. A correlation analysis showed that satDNAs with longer unit length showed higher A+T content ($r= 0.65$, $P= 0.031$).

Contamination coefficient calculation

The *de novo* assembly of the two RNA-Seq libraries yielded 85,246 contigs with N50= 1,953 nt for the sporophyte, and 347,685 contigs with N50= 782 nt for the gametophyte, the

316 latter showing four times more contigs than the former thus showing much higher diversity of
317 transcripts in the gametophyte, which raised our suspicions of possible contamination.
318 Annotation with SwissProt revealed the existence of 17,224 contigs in the sporophyte
319 sharing terms with those found in the gametophytic transcriptome and, to test the existence
320 of putative contamination, we selected a random sample including 500 of these contigs.
321 Blast2GO annotated 488 of them, 96% of which showed top similarity with Viriplantae, 1%
322 with Bacteria, 2% with Fungi and 1% with Metazoa. On the other hand, we got 77,772
323 gametophytic contigs with annotation terms being absent in the sporophyte library, 672 of
324 which mapped in both gametophytic gDNA libraries (VALDg and ALMOg). Blast2GO annotated
325 665 of them and, remarkably, only 16% of them annotated with Viriplantae (in high contrast
326 with the 96% observed for the contigs shared with the sporophyte), whereas 7% did with
327 Bacteria, 16% with Fungi, 45% with Metazoa and 16% with other Eukaryota. These results
328 indicate that DNA extraction in the gametophytes resulted severely contaminated in spite of
329 careful cleaning (see methods).
330 To get an estimate of the contamination level in the gametophyte gDNA libraries, we
331 estimated copy number for 623 sporophytic contigs being longer than 3000 nt. The average
332 copy number was 0.92, 0.91, 0.30 and 0.51 for OJENs, VALDs, VALDg and ALMOg, respectively
333 (Table S2), with remarkably lower values in the gametophyte libraries. Assuming that the lower
334 copy number for these contigs in the gamethophytes is due to coverage decrease caused by
335 the presence of contaminants, we normalized copy numbers in respect to the highest value
336 (that in OJENs) and obtained coefficients (1 in OJENs, 0.98 in VALDs, 0.32 in VALDg and 0.55 in
337 ALMOg) which were used for correcting genomic abundance of satDNA (Table 1).
338
339 ***satDNA abundance and divergence in the context of other repetitive DNAs***
340 Collectively, all 11 satDNAs represent between 0.43% and 0.33% of the genome of *V.*
341 *speciosa* depending on the library (Table 1 and Figure S1). There were some differences
342 between libraries in the abundance for certain satDNAs, but a Friedman ANOVA comparing
343 abundances for the 11 satDNAs between the four libraries did not reach significance (χ^2=7.57,
344 N=11, df=3, P=0.056). This indicates that some specific satDNAs have recently been
345 differentially amplified in a given population but not in others, but there is no general
346 tendency for all satDNAs as a whole, except for OJENs showing higher abundance for 5
347 satDNAs (VspSat01-59, VspSat03-33, VspSat06-67, VspSat07-70 and VspSat11-34) but lower
348 abundance for only one (VspSat04-107). Therefore, OJENs showed the highest figure for total
349 satDNA abundance (0.43% compared with 0.36%, 0.33% and 0.37% in VALDs, VALDg and

ALMOg, respectively). However, we found significant differences between the four libraries in respect to satDNA divergence (Friedman ANOVA: χ^2=13.73, N=11, df=3, P=0.0033), with OJENs showing the lowest divergence (Figure S3). This result would be consistent with the fact that the higher abundance found in OJEN was due to recent amplifications decreasing divergence for certain satDNAs.

No significant correlation was found between satDNA abundance and divergence within each library (P= 0.632 in OJENs, P= 0.697 in VALDs, P= 0.692 in VALDg and P= 0.563 in ALMOg). Likewise, abundance and divergence failed to show significant correlation with unit length or A+T content (see Table S3).

Telomere sequences were not found through the SatMiner approach. Notwithstanding, several thousands of telomeric repeats were found by searching TTTAGGG patterns among NGS reads. RepeatMasker analysis showed that the abundance of telomere sequences was 0.0256% and 0.0254% in OJENs and VALDs, respectively.

In addition, by using the "simple repeats" option of RepeatMasker, we found 1.77% microsatellite abundance in OJENs and 2.02% in VALDs, but a t-test for dependent samples showed that this difference is not significant (t= 1.08, df= 5, P= 0.33). Likewise, a comparison of microsatellite divergence between OJENs and VALDs failed to show significant difference (*t*= 1.19, df= 5, P= 0.29). In case of telomeric and microsatellite repeats, we did not used the gametophyte gDNA libraries because contamination would yield misleading abundance estimates given that their extremely short motives could not be distinguishable with those of the contaminants.

On the other hand, the RepeatExplorer output showed 50,53% TE genomic abundance in OJENs and 49,86% in VALDs. A description of the different TE classes found within the genome of *V. speciosa* is listed in Table 2. Repeats classified as LTR-retrotransposons represented the major fraction of the genome of *V. speciosa*, comprising up to ~28% of their nuclear DNA. They were mostly represented by Ty3/gypsy elements (Table 2). Ty1/copia elements were generally less abundant (~11,5% of the genome). Other mobile elements detected included LINEs (non-LTR retrotransposons) which represent between 3,86% and 3,62% of the genome in OJENs and VALDs, respectively. On the other hand, DNA transposons, mainly those of the CACTA superfamily, represent about the 3,7% of the genome. Unfortunately, there were another 14% of repetitive sequences (transposable elements according to the graph-based clustering) that were not specifically annotated.

Intrapopulation satDNA sequence variation

Figure 1 displays repeat landscape plots representing, for each satDNA, abundance (Y axis) and divergence (X axis) with respect to a consensus sequence built for each satDNA repeat unit. Bearing in mind that satDNA evolution may be mainly marked by amplification and homogenization processes (both decreasing divergence) and point mutations (increasing divergence), the profiles of repeat landscapes result highly informative on the age of satDNA variants within a same family. It is thus reasonable to infer that peaks at lower divergence values are the product of recent amplification or homogenization, whereas those at higher divergence values are probably older variants degenerated by accumulation of mutations. Consistently, telomeric repeats showed two peaks, one corresponding to extremely low divergent sequences, as expected for sequences generated by the active role of telomerase, and the other, at about 15% divergence, suggesting the existence of ectopic telomere tandem repeats which are not under telomerase action and thus manifest high divergence (Figure 1). Likewise, VspSat01-59 showed two types of abundant repeats differing in divergence, suggesting that they might show different ages or else differential tendencies to homogenization. Out of the remaining satDNAs, VspSat06-67 showed the lowest divergence (i.e. the highest homogenization), as indicated by a main peak below 5% divergence. On the other hand, VspSat02-101, VspSat03-33, VspSat05-141 and VspSat08-82 showed a main peak between 5% and 10% divergence, whereas VspSat04-107, VspSat07-70, VspSat09-68, VspSat10-62 and VspSat11-34 showed very flat distributions suggesting the presence of a broad range of sequence variations in respect to the consensus (Figure 1).

Interestingly, microsatellite landscape plots also showed two peaks, one corresponding to extremely low divergent sequences in homogeneous loci, probably of recent origin, and the other at about 20% divergence pointing to the existence of loci including old repeats degenerated by mutation (Figure S4).

SatDNA sequence divergence was low between populations

Due to the fact that most satDNA families in this species showed repeat unit lengths lower than Illumina read length, we were able to extract a number of monomers directly from the reads, thus resembling a massive cloning experiment. This rendered a total of 1,045 repeat units, even though the number of monomers obtained for the longest satDNAs (e.g. VspSat04-107 and VspSat05-141) was low because they depended on overlapping read pairs (Table S4). With these data, differences between populations were similar, or even lower, to the intra-population variation observed for each satDNA (not shown). Likewise, phylogenies for repeat sequences did not display differentiation between populations (not shown). In fact, the

418 sequences appeared intermingled in the phylogenetic trees independently of population of
419 origin.
420
421 ***Conserved motives and satDNA curvature***
422 An analysis of nucleotide diversity (π) per position in each satDNA showed that π
423 sharply varied between positions, with similarly alternating peaks and valleys. Interestingly,
424 several satDNA graphs showed the existence of conserved parts, with little o no variation,
425 within repeat units. For instance, positions 49-59 in VspSat02-101, 46-55 in VspSat04-107 and
426 106-124 in VspSat05-141 were extremely conserved compared to the remaining nucleotides in
427 each of these satDNA units (Table S5 and Figure S5). Figure 2 includes sequence logos for each
428 satDNA which clearly convey level of sequence divergence and reveal the conserved motives.
429 The position of the conserved motif coincided with a peak of DNA curvature in the case of the
430 VspSat04-107 satDNA (Figure S6). The curvature-propensity plot contains one peculiar
431 maximum in this region whose magnitude (17.8 degrees/10.5 bp helical turn) roughly
432 corresponds to the value calculated for other highly curved motifs (Goodsell and Dickerson,
433 1994). Therefore, we believe that this region may adopt a curved conformation. The conserved
434 regions in the VspSat02-101 and VspSat05-141 satDNAs were not within a peculiar maximum
435 peak of curvature. However, the same plot drawn with the consensus bendability scale
436 showed a conspicuous peak in this region in both cases, with a curvature-propensity plot
437 showing peaks in positions 20-40 (13.1 degrees/10.5 bp helical turn) and 28-36 (10
438 degrees/10.5 bp helical turn) within the VspSat02-101 and VspSat05-141 units, respectively
439 (not shown). In addition, the VspSat08-82 satDNA showed two conspicuous peaks of curvature
440 propensity >15 degrees/10.5 bp helical turn. However, curvature-propensity plots failed to
441 show any value indicative of strong curvature for the remaining satDNA families. None of the
442 conserved motifs were found to be significantly related to any other known DNA-binding
443 motif.
444
445 ***Similarity between satDNA families***
446 Some satDNA families showed complex units including subrepeats showing high
447 percentages of similarity with other shorter families. For instance, the VspSat06-67 unit
448 includes two direct subrepeats of 25 bp between positions 7-31 and 40-64 (76% identity), each
449 showing high similarity (64% and 68%) with the core of the 34 bp repeat of the VspSat11-34
450 satDNA unit (Figure 3). VspSat10-62 satDNA units are a rearranged version of the VspSat09-68
451 monomers with a 6 bp deletion (75% identity; 83.3% identity in the matched part of the

sequence) (Figure 4). The VspSat01-59 satDNA is also interesting by including a complex combination of trinucleotides according to the formula variable sequence-$(GAT)_2(GTG)(GAT)_3(GTG)TC(GAT)_4(GTG)TC$-variable sequence, whereas the VspSat03-33 satDNA is composed of three repetitions of a simplified version of the former formula: $(GAT)_2(GTG)GC$, showing 87% of identity with VspSat01-59 (Figure 5). Finally, the VspSat08-82 satDNA showed units composed of two parts, each one being a palindrome (Figure S7). Prediction of the lowest free energy structure and the structure generated from highly probable base pairs for VspSat08-82 sequence revealed a particular capability to acquire cruciform structures of VspSat08-82 monomers (Figure S7). Finally, the complex structure observed for most satDNAs analyzed here, except VspSat02-101, VspSat04-107 and VspSat05-141, implied sequences showing a high probability to acquire particular secondary structures (not shown). These data support the consideration of the existence of some satDNA superfamilies (SF), derived from a common ancestor satDNA, in *V. speciosa* by showing sequence homology, such as VspSat01-59 and VspSat03-33 (SF1), VspSat06-67 and VspSat11-34 (SF2) and VspSat09-69 and VspSat10-62 (SF3).

Discussion

A short catalogue of short but complex satDNAs in a large genome

Next Generation Sequencing (NGS) and high-throughput *in silico* analysis of the information contained in NGS reads (Novák et al., 2013, 2017; Ruiz-Ruano et al., 2016) have overtaken the limitation of conventional methods for the identification of the satDNA profile of *V. speciosa* by which the satellitome has been elusive during years in this species (Garrido-Ramos, personal observation). This is probably because the percentage that each of these satDNAs in the genome is scarce enough to be unperceived (Table 1 and Figure S1). In fact, satDNA is not an abundant fraction of the repetitive part of the genome in *V. speciosa* (about 0,4% of the genome), in spite of its large genome size (10.496 Gb; Obermayer et al., 2002) and in high contrast with other species (Ambrožová et al., 2011; Garrido-Ramos, 2015, 2017; Melters et al., 2013). However, this value is even higher than those found in a set of six leptosporangiate ferns from across a range of three major clades (Polypodiales, Cyatheales and Gleicheniales), where Wolf et al. (2015) found that satDNA represents 0.1 ± 0.03% (mean ± SE) of these fern genomes. These authors remarked that this satDNA abundance found in ferns is lower than that found in a group of six selected seed plants (0.8 ± 0.34%), while the abundance of individual satDNA families in seed plants actually varies from 0.1% to 36%, according to data gathered from non genomic approaches (Garrido-Ramos, 2015, 2017). No satDNA family

reaches 0.1% of the genome in the case of *V. speciosa* (see Table 1). The presence of so scarce set of satDNA in a species with such a large genome is thus intriguing, and further research is needed at this respect. A possible explanation is that satDNA families of *V. speciosa* are young and have not yet had time to increase in abundance. This is in high contrast with the old age of this genus (Pryer et al., 2004), unless satDNA turnover is extremely fast in this species. This latter possibility appears to be unlikely given the resemblance in satDNA content and abundance between the three populations analyzed here, and the homology found between several families constituting superfamilies, suggesting that satDNA families are long-lived in this species. This is also supported by the existence of highly divergent variants for most satDNA families, evidenced by the repeat landscapes in Figure 1, suggesting that the rate of satDNA degeneration through point mutation is high in this species. Another possibility might be related to the existence of genomic constraints impeding satDNA accumulation. Thus, the alternation of long lasting haploid and diploid stages could run against the accumulation of high amounts of satDNA. For instance, satDNA amplification could be restrained during the haploid stage since unequal crossing-over would operate mainly during diploidy.

Alternatively, the active elimination of useless satDNA in *V. speciosa* might explain why this large genome contains such a low amount of satDNA. This might be due to a high rate of DNA removal in this species. Differential DNA loss is an interesting prospect which merits future investigation in *V. speciosa*, as it appears to be a programmed and regulated process in many eukaryote genomes involving satDNA diminution from germ to somatic lines (Wang and Davis 2014). However, we have not found significant satDNA amount differences between the haploid and the diploid phases of *V. speciosa*.

An important contribution of TEs to the large genome size of V. speciosa

The large genome of the fern *V. speciosa* is mainly populated by TEs (~50% of the genome; Table 2), in contrast with the extremely low amounts of satDNA representing only ~0,4% of the genome. TEs are highly ubiquitous elements found in all kingdoms of living organisms and are highly abundant in some genomes, reaching up to the 85% of some plant genomes, such as that in maize (Schnable et al., 2009). Furthermore, TE content can differ greatly even between related species, thus being the main responsible for genome size differences between them (Piegu et al., 2006; Hu et al., 2011). We have found a general landscape for repetitive DNA genomic composition in *V. speciosa* similar to that found in other plants (reviewed in López-Flores and Garrido-Ramos, 2012). In a recent analysis of six fern species from across a range of three major clades (Polypodiales, Cyatheales and Gleicheniales),

Wolf et al. (2015), found that, compared with seed plants, ferns had a higher proportion of DNA transposons and LINEs in their genomes. Likewise, we have also found a higher proportion of these two types of elements in *V. speciosa* (~3,7% in both cases) compared with those in seed plants (mean percentages: ~0,83% and ~0,89%, respectively) and even higher than those found in other ferns (mean percentages: ~3,2% and ~2,2%, respectively). Wolf et al. (2015) also revealed that LTR/copia and LTR/gypsy retrotransposons represent 14% and 15%, respectively, of fern genomes. Depending on the species, values ranged between 10% and 25% of the genome for LTR/copia and between 8% and 25% of the genome for LTR/gypsy. However, they did not find a correlation between genome sizes and LTR retrotransposon amounts (Wolf et al., 2015). The fraction of the genome that in *V. speciosa* is occupied by these elements is within those ranges: ~11,5% LTR/copia and 16% LTR/gypsy.

A+T content is higher in longer repeat units of satDNA

SatDNA varies widely among species not only in abundance but also in repeat length, repeat sequence, and nucleotide composition (Melters et al., 2013; Plohl et al., 2012; Mehrotra and Goyal, 2014; Garrido-Ramos, 2015, 2017). Remarkably, all satDNA families found in *V. speciosa* are short and, most of them, A+T rich (see Table 1). In fact, in general, it has been found that satellite repeats are generally AT-rich, especially in the case of centromeric satellite DNAs (Garrido-Ramos, 2015). According to theoretical models of satDNA evolution and on the basis of experimental evidence any random sequence can lead to a family of tandem repeats (Smith, 1976; Melters et al., 2013). In this context, we should expect that average A+T content of the monomer collection comprising the satellitome (ignoring differential abundances caused by processes subsequent to satDNA origin) would reflect A+T content in the genome as a whole. In *V. speciosa*, average A+T content is 58.8% in the satellitome and 61.5% in the genome (inferred from the Illumina reads, not shown), i.e. 2.7% lower in the former. In the grasshopper *Locusta migratoria*, these figures differed by 6% suggesting a tendency for satDNA to arise from G+C rich regions (Ruiz-Ruano et al., 2016). In *V. speciosa*, A+T rich satDNAs represent almost two thirds of satDNA content (Table 1) and, likewise in *L. migratoria* (Ruiz-Ruano et al., 2016), there is a tendency for longer repeats to show higher A+T content (see Table 1). Therefore, a tendency to increase length and A+T content with age would bring satellitome A+T content close to A+T genomic average even though satDNA showed a tendency to rise up from G+C rich regions.

On the other hand, satDNA is subject to epigenetic modification such as the methylation of cytosines, so that deamination of 5-methylcytosines might contribute to the

554 relatively high A+T content of satDNAs in *V. speciosa*. Alternatively, the finding of lower A+T
555 content in the satellitome than in the genome of *V. speciosa* might be attributable to
556 procedural reasons, as it appears that the standard protocol for preparing Illumina libraries
557 (including PCR) might result in reduced representation of A+T rich satDNA in the final
558 sequences (Wei et a., 2018).
559
560 ***Repeat unit length tends to increase during satDNA evolution***
561 Plant satDNA sequences commonly have unit lengths of 135-195 bp or 315-375 bp, but
562 repeat-length might range between 58 bp of the pAm1 satDNA of *Avena* to the 5.9 Kb of the
563 2D8 repeats of *Solanum bulbocastanum* (Mehrotra and Goyal, 2014; Garrido-Ramos, 2015,
564 2017). Shorter monomer length has been found, for instance, for the 38 bp of the VicTR-B
565 satDNA DNA in *Vicia* (Macas et al., 2006). The case of *V. speciosa* is exceptional, at this respect,
566 because all satDNA families found show short repeat units (between 33 and 141 bp, with only
567 three families surpassing 100 bp).
568 Among the collection of satDNAs in *V. speciosa*, we found several complex satDNA
569 families that might guide us in the clarification of the apparently yet ongoing evolutionary
570 process for the formation of longer repeat units. The three superfamilies found illustrate this
571 point. For instance, SF3 is composed of VspSat09-69 and VspSat10-62, two homologous
572 satDNAs differing in a 7 bp indel. SF2 includes VspSat06-67 and VspSat11-34, the former being
573 composed of two divergent VspSat11-34 units thus being a higher-order repeat (HOR) of the
574 latter. Finally, SF1 is also composed of two satDNA families, so that VspSat01-59 includes two
575 subrepeats derived from divergent VspSat03-33 units, the former being also a HOR of the
576 latter. This last case is enlightening as both satDNAs are composed of shorter sub-repeats of
577 complex combinations of trinucleotides, an indication of the implication of two different
578 mechanisms acting at different times: replication slippage (Garrido-Ramos, 2015, 2017) might
579 be in the origin of the shorter units of VspSat03-33 whereas the longer satDNA (VspSat01-59)
580 might have been originated by unequal crossing-over (Garrido-Ramos, 2015, 2017). These two
581 satDNAs, as well as the VspSat06-67 and the VspSat11-34 appear to be in an ongoing process
582 of amplification in the OJEN population. The combination of short repeat units into longer
583 units constituting HORs is a common trend in satDNA evolution (Plohl et al., 2008; Garrido-
584 Ramos, 2017). We could thus postulate that longer satDNAs in *V. speciosa* evolve from shorter
585 ones by means of alternate cycles of duplication and divergence, as previously proposed for
586 other satDNA families (Navajas-Pérez et al., 2005; Macas et al., 2006; Emadzade et al., 2014).

We have checked the genomic content of microsatellites in *V. speciosa* to test whether they were conceivable seeds for longer satDNA repeat units. We found an important contribution of different types of microsatellites to the genome content of *V. speciosa*. Indeed, depending on population, there was between four and five times more microsatellite than satDNA content in this genome, suggesting that the former might be a source for new satDNAs. Recently, Wolf et al. (2015) found that microsatellites represent 15.5 ± 1.5% of the genome in six fern species, a much higher figure than that reported for seed plants (1.19 ± 0.89%). However, Portis et al. (2016), obtained even lower values for different seed plants (0.17%-0.67%). The case of *V. speciosa* (1.77-2.02%) is thus closer to seed plants than to the six fern species analyzed by Wolf et al. (2015).

Structural features in V. speciosa satDNAs

Structural features of satDNA might have implications on functional constraints. In this respect, VspSat02-101, VspSat04-107 and VspSat05-141 satDNAs share several interesting features. They are composed by the longer satDNA repeat units, are A+T rich, are among the most abundant satDNAs and are among the most homogeneous satDNAs, at least the VspSat02-101 and the VspSat05-141 satDNA families. In addition, they also share structural characteristics of bendability and curvature propensity and, interestingly, bend and curvature conspicuous peaks coincide in these repeats with the location of highly conserved motifs within VspSat02-101, VspSat04-107 and VspSat05-141 monomers.

Epigenetic control of heterochromatin assembly by transcriptional silencing complexes (RITS), recruitment of histone methyltransferases, histone H3 methylation (H3K9me2), and recruitment of heterochromatin protein 1 (HP1) is well documented (Pezer et al., 2012; Plohl et al., 2012; Johnson et al., 2017). The capability of DNA stretches to bend and curve into a super-helical tertiary structure is a sequence-dependent property that has been proposed many times as an additional element involved in specific recognition of DNA-binding protein components of the heterochromatin, which might facilitate the tight packing of DNA into heterochromatin (reviewed in Plohl et al., 2012; Pezer et al., 2012).

On the other hand, the VspSat08-82 repeats are the result of two consecutive palindromes which, in combination, give the repeats the capability to acquire particular secondary structures such as cruciform structures. Cruciform structures are targets for many architectural and regulatory proteins and are fundamentally important for a wide range of biological processes, including replication, regulation of gene expression, nucleosome structure and recombination (see, for example, the review of Brázda et al., 2011). The most

621 remarkable detected inverted repeats are found in satDNAs from *Tribolium* species,
622 characterized by complex monomers composed of inversely oriented subunits capable of
623 forming large dyad structures relevant in the formation of heterochromatin architecture in
624 these species and in the amplification processes of these types of satDNAs (Plohl, 2010).
625
626 ***No apparent concerted evolution***
627 Our data reveal no apparent genetic differentiation, i.e. concerted evolution (Garrido-
628 Ramos, 2015, 2017), of satDNAs between the three populations analyzed since the three
629 populations share the same library with similar abundances and only decreased divergence in
630 certain satDNAs in OJEN. Likewise, nucleotide diversity was about similar at intra- and
631 interpopulation levels. The absence of concerted evolution might be due to recent common
632 descent of the three populations and/or frequent gene flow between populations. Recently,
633 Ben-Menni Schuler et al. (2017) have found support for migration-drift equilibrium in these
634 populations, suggesting that gene flow had a key influence on population structure although
635 populations are currently predominately influenced by genetic drift. In addition, as mentioned
636 before, unequal crossing-over should operate mainly during diploidy and the alternation of
637 long lasting haploid and diploid stages could run against sequence homogenization.
638 On the other hand, according to this model, it might be expected that, in the absence
639 of sexual reproduction, the haploid population (ALMO) should have higher levels of sequence
640 variation for satDNAs (Luchetti et al., 2003; Plohl et al., 2008). Data suggested that evolution of
641 satDNA in ants follows a concerted evolution pattern but that this process is slow in relation
642 with other organisms, probably due to the eusociality and haplodiploidy of these insects
643 (Lorite et al., 2017). In the thelytokous partenogenetic species of the genus *Bacillus*, Luchetti et
644 al. (2003) found that sexuality acts as a driving force in the fixation of sequence variants within
645 a satDNA family thus generating intrapopulation cohesiveness and interpopulation
646 discontinuities, and that parthenogenesis has a slowing effect on molecular turnover
647 processes. However, the analysis also proved the spreading of new variants in unisexual
648 specimens by gene conversion events arriving at the conclusion that given enough time,
649 sequence homogenization can take place in a unisexual species. The study also confirmed the
650 mitotic plasticity of tandem repeats since, to accomplish this observation, gene conversion
651 events should preferentially take place during cell division. It appears that the haploid ALMO
652 population seems to mirror this situation. A similar context is found for satDNAs of Y
653 chromosomes of the plant *Rumex acetosa*. While the Y chromosomes of *R. acetosa* do not
654 recombine, sister-chromatid interchanges should explain gene conversion homogenizing

events which should lead to concerted evolution of Y-linked satDNA DNA subfamilies (Navajas-Pérez et al., 2006).

A warning on possible contamination of DNA extractions

In this paper, we have developed a reliable and successful protocol of evident utility for testing the possible existence of contaminations during DNA extraction for high throughput sequencing methods. As a preventive measure, we thought that the gametophyte samples, by living in close association with ground and water, could be contaminated even with very high standards of carefully and exhaustive isolation and cleaning of the filaments. This allowed us to overpass any possible pitfall when quantifying satDNA abundance in these samples since, without the application of this corrective calculations, we would have estimated higher amounts of satDNA in sporophytes than in gametophytes, with the consequent impact on key concepts such as satDNA gain/loss between different lifecycle phases. The application of our method for the obtention of correction coefficients, and their use in our calculations, allowed us to find more reliable estimates of satDNA abundance in every sample of *V. speciosa*. In addition, our estimates are independent of the percentage of contamination in each sample because the coefficients were devised in terms of relative presence of a high number of long contigs (>3000 nt, thus increasing the likelihood of nucleotide mapping), which were used as reference, in resemblance to the use of reference genes for quantitative PCR.

Concluding remarks

There is a trend for longer (and older) satellites in *V. speciosa* to show higher A+T content and to evolve from shorter ones. In this context, the role of microsatellites in the formation of some of these satDNAs is striking. The contributions of satDNA (~0.4%) and microsatellites (~2%) to the large genome of *V. speciosa* are almost negligible compared to that of TEs (~50%). TE composition in this species, like in other ferns, was about similar to that in seed plant species, except for a higher proportion of DNA transposons and LINEs in the former. Our results also suggest that reproduction mode or phase alternation between long lasting haploid and diploid stages does not influence satDNA abundance or divergence. Finally, from a methodological point of view, our proposal of a reliable and successful protocol for testing, and dismiss in satDNA quantification, the existence of unavoidable contaminants, might be useful for other NGS studies.

Acknowledgments: This research has been financed by the Spanish Ministerio de Economía y Competitividad and FEDER founds, grant: CGL2010-14856 (subprograma BOS). The Dirección General de Gestión del Medio Natural y Espacios Protegidos of the Consejería de Medio Ambiente y Ordenación del Territorio de la Junta de Andalucía authorized and facilitates the sampling of the material. We are highly indebted to Carmen Rodríguez Hiraldo and to Jaime Pereña Ortiz who, together the team of Agentes de Medio Ambiente of the Consejería, helped us with the sampling procedure.

References

Altschul SF, Madden TL, Schäffer AA, Zhang J, Zhang Z, Miller W, Lipman DJ. 1997. Gapped BLAST and PSI-BLAST: a new generation of protein database search programs. *Nucleic Acids Research* **25**: 3389-3402.

Ambrožová K, Mandáková T, Bureš P, Neumann P, Leitch IJ, Koblížková A, Macas J, Lysak MA. 2011. Diverse retrotransposon families and an AT-rich satellite DNA revealed in giant genomes of *Fritillaria* lilies. *Annals of Botany* **107**: 255-268.

Bairoch A, Apweiler R. 2000. The SWISS-PROT protein sequence database and its supplement TrEMBL in 2000. *Nucleic Acids Research* **28**: 45-48.

Ben-Menni Schuler SBM, García-López MC, López-Flores I, Nieto-Lugilde M, Suárez-Santiago VN. 2017. Genetic diversity and population history of the Killarney fern, *Vandenboschia speciosa* (Hymenophyllaceae), at its southern distribution limit in continental Europe. *Botanical Journal of the Linnean Society* **183**: 94-105.

Biscotti MA, Olmo E, Heslop-Harrison JS. 2015. Repetitive DNA in eukaryotic genomes. *Chromosome Research* **23**, 415–420.

Bolger AM, Lohse M, Usadel, B. 2014. Trimmomatic: a flexible trimmer for Illumina sequence data. *Bioinformatics* **30**: 2114-2120.

Brázda et al. 2011. Cruciform structures are a common DNA feature important for regulating biological processes; *BMC Mol Biol* **12**: 33.

Brukner I, Sánchez R, Suck D, Pongor S. 1995. Sequence dependent bending propensity of DNA as revealed by DNAse I: Parameters for trinucleotides. *EMBO Journal* **14**: 1812-1818.

Conesa A, Götz S, García-Gómez JM, Terol J, Talón M, Robles M. 2005. Blast2GO: a universal tool for annotation, visualization and analysis in functional genomics research. *Bioinformatics* **21**: 3674-3676.

Drummond AJ et al., 2009. Geneious v. 4.8 Biomatters Ltd. Aukland, New Zealand.

Emadzade K, Jang TS, Macas J, Kovařík A, Novák P, Parker J, Weiss-Schneeweiss H. 2014. Differential amplification of satellite PaB6 in chromosomally hypervariable *Prospero autumnale* complex (Hyacinthaceae). *Annals of Botany* **114**: 1597-1608.

Gabrielian A, Pongor S. 1996. Correlation of intrinsic DNA curvature with DNA property periodicity. *FEBS Letters* **393**: 65-68.

Garrido-Ramos MA. 2015. Satellite DNA in Plants: More than Just Rubbish. *Cytogenetics and Genome Research* **146**: 153-170.

Garrido-Ramos MA. 2017. Satellite DNA: An Evolving Topic. *Genes* **8**: pii E230.

Goodsell DS, Dickerson RE, 1994. Bending and curvature calculations in B-DNA. *Nucleic Acids Research* **22**: 5497-5503.

Haas BJ, Papanicolaou A, Yassour, M, Grabherr M, Blood PD, Bowden J. et al. 2013. *De novo* transcript sequence reconstruction from RNA-seq using the Trinity platform for reference generation and analysis. *Nature Protocols* **8**: 1494.

Hu TT et al. 2011. The *Arabidopsis lyrata* genome sequence and the basis of rapid genome size change. *Nature Genetics* **43**: 476-481.

Johnson WL, Straight AF. 2017. RNA-mediated regulation of heterochromatin. *Current Opinion in Cell Biology* **46**: 102-109.

Kent WJ. 2002. BLAT—the BLAST-like alignment tool. *Genome Research* **12**: 656-664.

Kim YB, Oh JH, McIver LJ, Rashkovetsky E, Michalak K, Garner HR, Kang L, Nevo E, Korol AB, Michalak P. 2014. Divergence of *Drosophila melanogaster* repeatomes in response to a sharp microclimate contrast in Evolution Canyon, Israel. *Proceeding of the National Academy of Science USA* **111**:10630-10635.

Librado P, Rozas J. 2009. DnaSP v5: a software for comprehensive analysis of DNA polymorphism data. *Bioinformatics* **25**: 1451-1452.

López-Flores I, Garrido-Ramos MA. 2012. The repetitive DNA content of eukaryotic genomes. *Genome Dynamics* **7**: 1-28.

Lorite P, Muñoz-López M, Carrillo JA, Sanllorente O, Vela J, Mora P, Tinaut A, Torres MI, Palomeque T. 2017. Concerted evolution, a slow process for ant satellite DNA: Study of the satellite DNA in the *Aphaenogaster* genus (Hymenoptera, Formicidae). *Organisms Diversity and Evolution* **17**: 595-606.

Luchetti A, Cesari M, Carrara G, Cavicchi S, Passamonti M, Scali V, Mantovani B. 2003. Unisexuality and molecular drive: Bag320 sequence diversity in Bacillus taxa (Insecta Phasmatodea). *Journal of Molecular Evolution* **56**: 587-596.

Macas J, Navrátilová A, Koblížková A. 2006. Sequence homogenization and chromosomal localization of VicTR-B satellites differ between closely related Vicia species. *Chromosoma* **115**: 437-447.

Melters DP, Bradnam KR, Young HA, Telis N, May MR, Ruby JG, Sebra R, Peluso P, Eid J, Rank D. et al. 2013. Comparative analysis of tandem repeats from hundreds of species reveals unique insights into centromere evolution. *Genome Biology* **14**: R10.

Mehrotra S, Goyal V. 2014. Repetitive sequences in plant nuclear DNA: Types, Distribution, Evolution and Function. *Genomics, Proteomics and Bioinformatics* **12**: 164-171.

Navajas-Pérez R, de la Herrán R, Jamilena M, Lozano R, Ruiz Rejón CR, Ruiz Rejón M, Garrido-Ramos MA. 2005. Reduced rates of sequence evolution of Y-linked satellite DNA in *Rumex* (Polygonaceae). *Journal of Molecular Evolution* **60**: 391-399.

Navajas-Pérez R, Schwarzacher T, de la Herrán R, Ruiz Rejón C, Ruiz Rejón M, Garrido-Ramos MA. 2006. The origin and evolution of the variability in a Y-specific satellite-DNA of Rumex acetosa and its relatives. *Gene* **368**: 61-71.

Navarro-Domínguez B, Ruiz-Ruano FJ, Cabrero J, Corral JM, López-León MD, Sharbel TF, Camacho JPM. 2017. Protein-coding genes in B chromosomes of the grasshopper *Eyprepocnemis plorans*. *Scientific Reports* **7**: 45200.

Novák P, Ávila Robledillo P, Koblížková A, Vrbová I, Neumann P, Macas J. 2017. TAREAN: A computational tool for identification and characterization of satellite DNA from unassembled short reads. *Nucleic Acids Research* **45**: e111.

Novák P, Neumann P, Macas J. 2010. Graph-based clustering and characterization of repetitive sequences in next-generation sequencing data. *BMC Bioinformatics* **11**: 378.

Novák P, Neumann P, Pech J, Steinhaisl J, Macas J. 2013. RepeatExplorer: a galaxy-based web server for genome-wide characterization of eukaryotic repetitive elements from next-generation sequence reads. *Bioinformatics* **29**: 792-793.

Obermayer R, Leitch IJ, Hanson L, Bennett MD. 2002. Nuclear DNA C-values in 30 species double the familial representation in pteridophytes. *Annals of Botany* **90**: 209-217.

Pezer Z, Brajković J, Feliciello I, Ugarković Đ. 2012. Satellite DNA-Mediated Effects on Genome Regulation. *Genome Dynamics* **7**: 153-169.

Piegu B et al. 2006. Doubling genome size without polyploidization: Dynamics of retrotransposition-driven genomic expansions in *Oryza australiensis*, a wild relative of rice. *Genome Research* **16:**, 1262-1269.

Plohl M. 2010. Those mysterious sequences of satellite DNAs. *Periodicum Biologorum* **112**: 403-410.

Plohl M, Luchetti A, Meštrović N, Mantovani B. 2008. Satellite DNAs between selfishness and functionality: Structure, genomics and evolution of tandem repeats in centromeric (hetero)chromatin. *Gene* **409**: 72-82.

Plohl M, Meštrović N, Mravinac B. 2012. Satellite DNA evolution. *Genome Dynamics* **7**: 126-152.

Portis E, Portis F, Valente L, Moglia A, Barchi L, Lanteri S, Acquadro A. 2016. A genome-wide survey of the microsatellite content of the globe artichoke genome and the development of a web-based database. *PLoS One* **11**: e0162841.

Pryer KM, Schuettpelz E, Wolf PG, Schneider H, Smith AR, Cranfill R. 2004. Phylogeny and evolution of ferns (monilophytes) with a focus on the early leptosporangiate divergences. *American Journal of Botany* **91**: 1582-1598.

Reuter JS, Mathews DH. 2010. RNAstructure: software for RNA secondary structure prediction and analysis. *BMC Bioinformatics* **11**: 129.

Rice P, Longden I, Bleasby A. 2000. EMBOSS: The European Molecular Biology Open Software Suite. *Trends in Genetics* **16**: 276-277.

Ruiz-Estévez M, Bakkali M, Martín-Blázquez R, Garrido-Ramos MA. 2017a. Differential expression patterns of MIKCC-type MADS-box genes in the endangered fern *Vandenboschia speciosa*. *Plant Gene* **12**: 50-56.

Ruiz-Estévez M, Bakkali M, Martín-Blázquez R, Garrido-Ramos MA. 2017b. Identification and characterization of TALE homeobox genes in the endangered fern *Vandenboschia speciosa*. *Genes* **8**: 275.

Ruiz-Ruano FJ, López-León MD, Cabrero J, Camacho JPM. 2016. High-throughput analysis of the satellitome illuminates satellite DNA evolution. *Scientific Reports* **6**: 28333.

Rumsey FJ, Vogel JC, Russell SJ, Barrett JA, Gibby M. 1999. Population genetics and conservation biology of the endangered fern *Trichomanes speciosum* (Hymenophyllaceae) in Scotland. *Biological Journal of the Linnean Society* **66**: 333-344.

Schmieder R, Edwards R. 2011. Fast identification and removal of sequence contamination from genomic and metagenomic datasets. *PLoS ONE* **6**: e17288.

Schnable PS et al. 2009. The B73 maize genome: Complexity, diversity, and dynamics. *Science* **326**: 1112-1115.

Smit AFA, Hubley R, Green P. 2015. RepeatMasker Open-4.0. 2013–2015. <http://repeatmasker.org>.

Smith GP. 1976. Evolution of repeated DNA sequences by unequal crossover. *Science* **191:** 528-535.

Suzuki K. 2013. Characterization of telomere DNA among five species of pteridophytes and bryophytes. *Journal of Bryology* **26**: 175-180.

Tamura K, Stecher G, Peterson D, Filipski A, Kumar S. 2013. MEGA6: Molecular Evolutionary Genetics Analysis version 6.0. *Molecular Biology and Evolution* **30**: 2725-2729.

Vlahovicek K, Kaján, Pongor S. 2003. DNA analysis servers: plot.it., bend.it, model.it and IS *Nucleic Acids Research* **31**: 3686-3687.

Wang J, Davis RE. 2014. Programmed DNA elimination in multicellular organisms. *Current Opinion in Genetics and Development* **27**: 26-34.

Wei KH, Lower SE, Caldas IV, Sless TJ, Barbash DA, Clark AG. 2018. Variable rates of simple satellite gains across the *Drosophila* phylogeny. *Molecular Biology and Evolution doi: 10.1093/molbev/msy005. [Epub ahead of print].*

Weiss-Schneeweiss H, Leitch AR, McCann J, Jang TS, Macas J. 2015. Employing next generation sequencing to explore the repeat landscape of the plant genome. In: Next Generation Sequencing in Plant Systematics Regnum Vegetabile; Hörandl, E., Appelhans, M., Eds.; Koeltz Scientific Books: Königstein, Germany, pp. 155–179.

Wolf PG, Sessa EB, Marchant DB, Li FW, Rothfels CJ, Sigel EM, Gitzendanner MA, Visger CJ, Banks JA, Soltis DE, Soltis PS, Pryer KM, Der JP. 2015. An exploration into fern genome space. *Genome Biology and Evolution* **7**: 2533-2544.

Figure legends

Figure 1. Repeat landscape plots representing, for each satDNA, abundance (Y axis) and divergence (X axis) with respect to a consensus sequence built for each satDNA repeat unit.

Figure 2. Sequence logos showing level of sequence divergence (from top to bottom: VspSat02-101, VspSat04-107 and VspSat05-141). Conserved motives are enclosed in a square.

Figure 3. Sequence comparison between the two parts of VspSat06-67 monomers and the VspSat11-34 monomers. Shaded areas represent conserved nucleotides between the three sequences.

Figure 4. Sequence comparison between VspSat09-68 and VspSat10-62 monomers. Shaded areas represent conserved nucleotides between the two sequences.

Figure 5. Sequence comparison between VspSat01-59 and VspSat03-33 monomers. Shaded areas represent conserved nucleotides between the two sequences.

Table 1. Characteristics of the 11 satDNAs found in *V. speciosa*.

Assembly/Cluster	Satellite name	Abundance (%)				Divergence (%)				Monomer lenght (nt)				AT (%)
		OJENs	VALDs	VALDg	ALMOg	OJENs	VALDs	VALDg	ALMOg	OJENs	VALDs	VALDg	ALMOg	
3/CL11	VspSat01-59	0.08	0.04	0.05	0.05	11.69	12.02	12.07	12.29	56-62	52-65	52-65	56-59	51.1
1/CL154	VspSat02-101	0.08	0.08	0.07	0.08	10.43	10.43	11.03	10.61	100-104	99-103	99-103	100-102	56.6
3/CL11	VspSat03-33	0.07	0.04	0.04	0.05	10.37	10.47	10.48	10.56	32-34	32-33	32-33	33-38	52.0
1/CL65	VspSat04-107	0.06	0.07	0.06	0.06	14.76	15.08	14.87	14.81	107	96-107	96-107	106-107	63.2
1/CL167	VspSat05-141	0.05	0.05	0.05	0.06	8.61	8.57	8.77	8.80	140-141	140-141	140-141	140-141	70.0
2/CL263	VspSat06-67	0.01	0.01	0.01	0.01	6.66	7.46	7.81	7.38	66-69	64-69	64-69	66-69	52.7
2/CL65	VspSat07-70	0.02	0.02	0.01	0.02	16.96	17.09	17.27	17.24	69-70	68-71	68-71	69-71	58.2
3/CL10	VspSat08-82	0.02	0.02	0.01	0.02	13.43	12.67	14.03	12.63	79-82	81-84	81-84	81-82	61.7
2/CL286	VspSat09-68	0.01	0.01	0.01	0.01	12.49	12.50	12.72	12.89	62-70	67-70	67-70	62-73	67.0
2/CL266	VspSat10-62	0.01	0.01	0.01	0.01	10.16	9.87	10.32	10.36	56-67	61-64	61-64	59-63	69.2
3/CL3	VspSat11-34	0.01	0.004	0.01	0.01	14.30	16.16	13.86	16.54	34-35	33-35	33-35	34	45.4
	Total	**0.43**	**0.36**	**0.33**	**0.37**									

Table 2. Contribution of TEs to the *V. speciosa* genome

	OJENs	VALDs
DNA	0,98%	1,13%
DNA/CACTA	2,44%	2,58%
DNA/hAT	0,16%	0,17%
LINE	3,86%	3,62%
LTR	0,76%	0.68%
LTR/Copia (Ty1)	11,46%	11,47%
LTR/Gypsy (Ty3)	16,53%	15,81%
ND	14,33%	14,41%
TOTAL	50,53%	49,86%

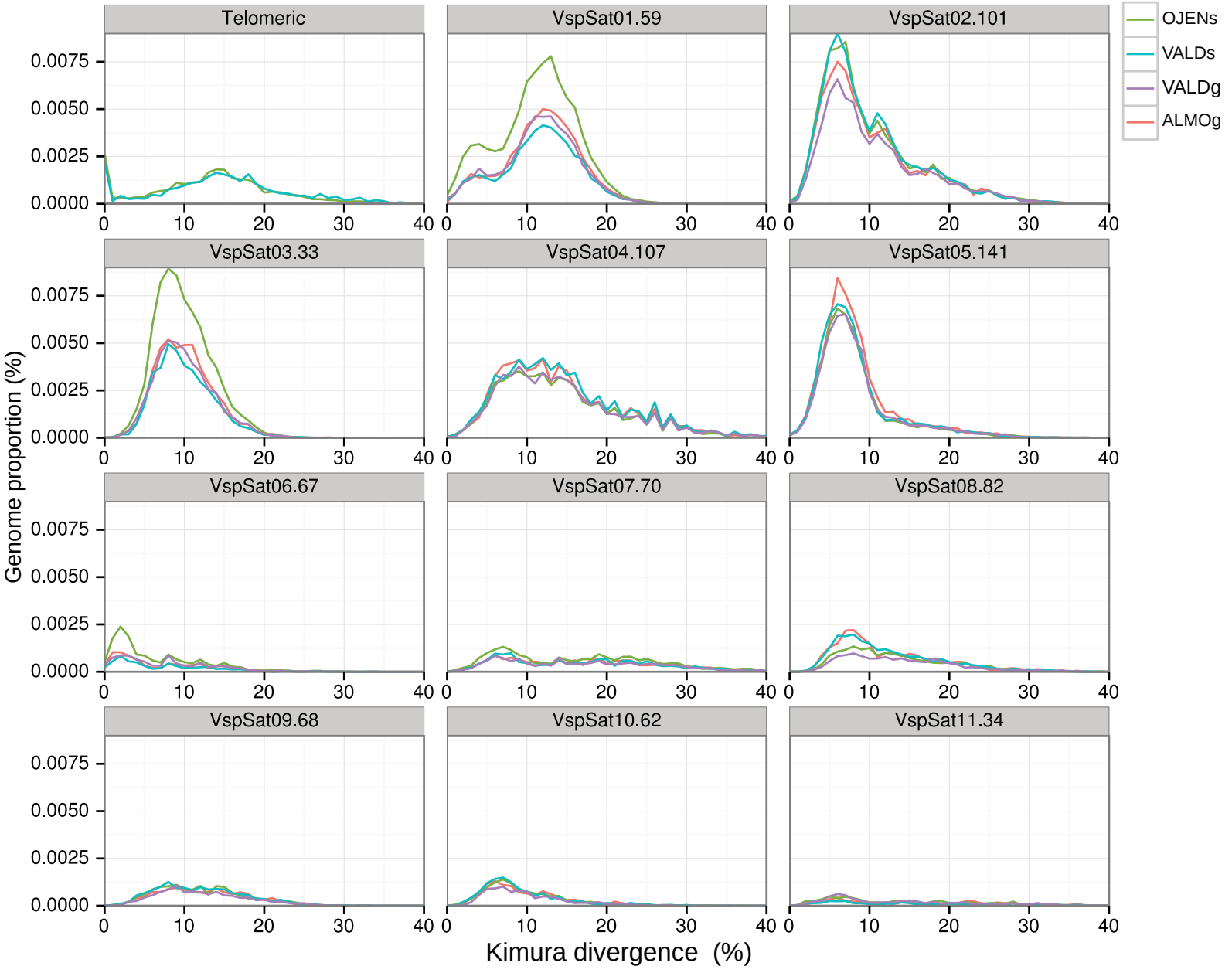
Telomeric
VspSat01.59
VspSat02.101
VspSat03.33
VspSat04.107
VspSat05.141
VspSat06.67
VspSat07.70
VspSat08.82
VspSat09.68
VspSat10.62
VspSat11.34
OJENs
VALDs
VALDg
ALMOg
Genome proportion (%)
0.0000
0.0025
0.0050
0.0075
0
10
20
30
40
Kimura divergence (%)

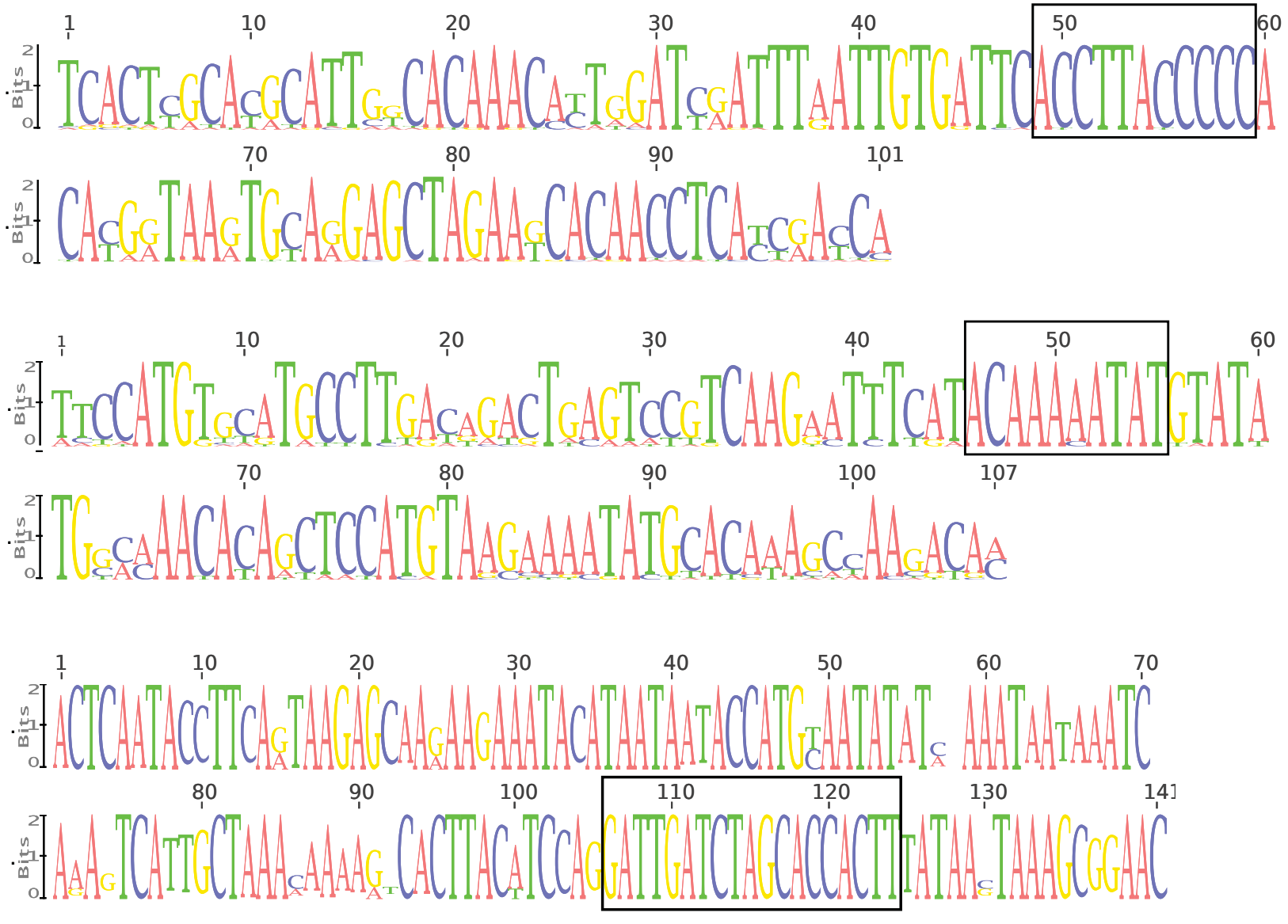
1
10
20
30
40
50
60
70
80
90
101
Bits
2
1
0
1
10
20
30
40
50
60
70
80
90
100
107
Bits
2
1
0
1
10
20
30
40
50
60
70
80
90
100
110
120
130
141
Bits
2
1
0

```
VspSat11-34     01TGTGTAGCCCATTCCAGGGGCCTTTCTTGCAACC
VspSat06-67-1   01TTTGTGGCTCATTCTTGGGGCCATATTTGCGGG 33
VspSat06-67-2   34CTGTTTGGTCATTCAAGGGGCCATTTGTGTGAGT67
```

VspSat11-34 *vs.* VspSat06-67-1: 65% identity
VspSat11-34 *vs.* VspSat06-67-2: 56% identity
VspSat06-67-1 *vs.* VspSat06-67-2: 65% identity

VspSat09-68:

CTATTTGTCTTTCTAATTGCTCATGATTAAAAGAAAGCTTTCAGCCATTGGGAGTTAGAATGATAATG

VspSat10-62:

CATTGGGAGTTGGAATGTTAATGTTATGAGTCTTTCAAATTGATTGAAAGAAAGCGTTTTAC

CTATTTGTCTTTCTAATTGCTCATGATTAAAAGAAAGCTTTCAGCCATTGGGAGTTAGAATGATAATG
TTATGAGTCTTTCAAAT------TGATTGAAAGAAAGCGTTTTACCATTGGGAGTTGGAATGTTAATG

```
VspSat01-59     CCCGCATGGATGATGTG--GATGATGATGTGTCGATGATGATGACGTGTCGATGGTGTGGG
VspSat03-33             GATGACGTGGCGATGAC---GTGGCGATGAT------GTGGC
```